EPJ manuscript No.
(will be inserted by the editor)

arXiv:0711.1703v2 [nucl-ex] 25 Jan 2008

Probing the nucleon structure with CLAS

Highlights of recent results.

Volker D. Burkert, for the CLAS collaboration.

Jefferson Lab, Newport News, Virginia, USA

February 2, 2008

Abstract. An overview of recent results with CLAS is presented with emphasis on the nucleon resonance program and related topics.

PACS. 1 1.55.Fv, 13.60.Le, 13.40.Gp, 14.20.Gk

1 Introduction

The beauty of the electromagnetic probe is that it allows us to efficiently address the central question of hadron physics: What are the relevant degrees of freedom at varying distance scales? Using electron beams we can vary the space-time resolution and momentum transfer to the nucleon independently. In doing so we probe the effective degrees of freedom in the nucleon from hadrons, constituent quarks, to elementary quarks and gluons. The study of nucleon resonance transitions, which is the focus of this workshop, provides a testing ground for our understanding of these effective degrees of freedom. Using the $SU(6) \otimes O(3)$ classification scheme of the symmetric constituent quark model (CQM), the known states can be sorted into supermultiplets of energy and orbital angular momentum of the 3-quark system. In this talk I will highlight some of the new CLAS results for the $N\Delta(1232)$ transition, and for some of the higher excited states of the nucleon. These data allow us to address questions about the underlying degrees of freedom of some of the well known states such as the Roper $P_{11}(1440)$, and $S_{11}(1535)$, both of which have also been presented using non-quark degrees of freedom. Studying the resonance transitions will allow us to make more definite statements about the nature of these states. Then I will discuss the well known problem of the "missing states", i.e. resonances predicted within the $SU(6) \otimes O(3)$ symmetry. Specific mass ranges are predicted in explicit models that break degeneracies through spin-spin interactions. However, many of these states have not been identified in experimental analysis. Going somewhat above the nucleon resonance region, there is also new information on the spin structure of the nucleon and the resulting effects on the parton distribution function from recent very precise CLAS data. Finally, I will briefly discuss the first DVCS results that cover a broad kinematics regime, and what we can learn from them about the generalized parton distributions (GPDs).

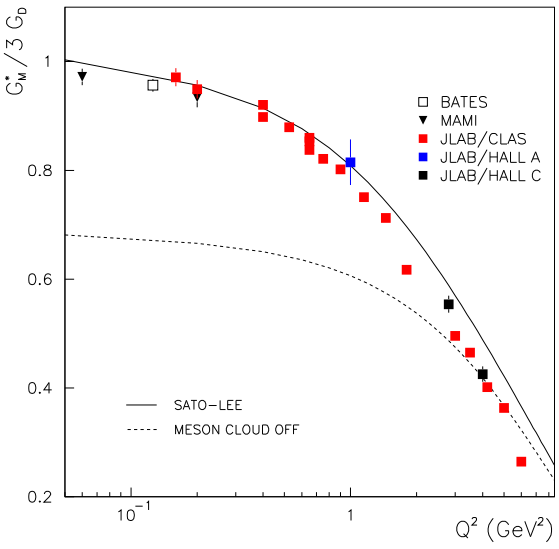


Fig. 1. Magnetic form factor for the $N\Delta$ transition.

2 The $N\Delta(1232)$ transition

The $N\Delta(1232)$ transition has been studied for more than 50 years with various probes. But only in the past decade have the experimental tools in electron scattering become available that enabled precise determinations of the magnetic transition form factor in π^0 production from protons with photon virtualities up to $Q^2 = 6$ GeV^2. Benchmark results from JLab [1,2,3,4], MIT-Bates [5], and MAMI [6] are shown in Fig. 1 relative to the dipole form which approximately describes the elastic magnetic form factor of

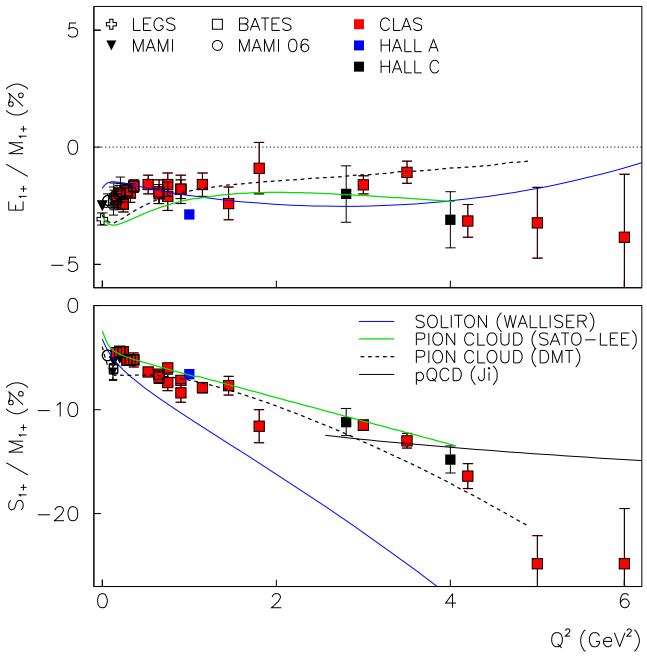


Fig. 2. The electric and scalar quadrupole ratios R_{EM} and R_{SM} for the $N\Delta$ transition.

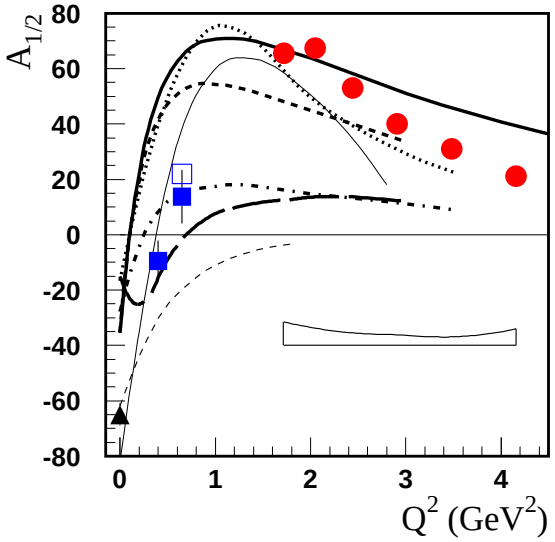


Fig. 3. The transverse transition amplitude $A_{1/2}$ in units of $10^{-3}GeV^{-1/2}$ for the Roper resonance, clearly showing the change in sign. The black triangle is the PDG average, the full squares are the results of single pion analysis, the open square represents the combined single and double pion analysis. The full circles are preliminary results from CLAS. The curves are predictions of quark model calculations discussed in ref. [8] with the exception of the thin dashed line which is the prediction of a hybrid baryon model.

the proton. The theoretical description in the Sato-Lee dynamical model includes dynamical pion contributions that are needed to explain the magnitude of G_M^* especially at lower Q^2. It is found that the pion contributions make up more than 30% of the total amplitude at the photon point, and remain sizeable even at the highest Q^2.

The electric and scalar quadrupole contributions, expressed as fractions of the magnetic dipole transition and given by the ratio $R_{EM} = Im(E_{1+})/Im(M_{1+})$ and the ratio $R_{SM} = Im(S_{1+})/Im(M_{1+})$, which are both shown in Fig. 2. R_{EM} remains small and negative even at the highest Q^2, in the range from -2% to -4%, and shows no indication of a trend towards the predicted asymptotic behavior of $R_{EM} \to +100\%$ at $Q^2 \to \infty$. Although R_{SM} shows a different behavior, and rises in magnitude with Q^2, it also shows no indication of approaching the predicted asymptotic behavior, $R_{SM} \to$ *constant* for $Q^2 \to \infty$. Both of these results present serious challenges to theory. One may expect that Lattice QCD (LQCD) will soon be able to calculate these ratios accurately up to high Q^2. First computations in quenched LQCD [7] have produced results at lower Q^2 that compare favorably with the measured R_{EM} values. However, they also reveal shortcomings for R_{SM} at the lowest Q^2 values where pion contributions are expected to be important and may be underestimated in quenched QCD.

3 The second resonance region

In the mass region above the $\Delta(1232)$ there are 3 excited nucleon states, the Roper $P_{11}(1440)$, the $S_{11}(1535)$ and the $D_{13}(1520)$. Each of these resonances has features that makes their investigation particularly interesting.

3.1 The Roper resonance, $P_{11}(1440)$

The $P_{11}(1440)$ is not a well understood state in the standard CQM. The mass is more than 100 MeV lower and the photocoupling amplitude has the wrong sign. Alternative models have been developed and make predictions for transition form factors, e.g. models using light cone dynamics [8] kinematics, or models describing the state as a hybrid baryon [9]. Other models that describe the state as a nucleon-meson molecule have been proposed but no transition form factors have been computed. The first systematic analyses of the Roper transition form factors was accomplished in a combined analysis of $n\pi^+$ and $p\pi^0$, and of $p\pi^+\pi^-$ electroproduction data from CLAS [10,11,12] that showed a rapid drop of the magnitude of the $A_{1/2}$ amplitude followed by a zero-crossing, while the longitudinal coupling $S_{1/2}$ is large and positive [13,14].

The non-relativistic QCM predicts an incorrect sign at the photon point and has no zero crossing, the light cone quark models give the correct sign at the photon point and predict the zero crossing, but lack strength at photon point. This is possibly related to contributions of the meson cloud which are not included in the light cone (LC) quark model calculations. Meson effects should be less important at higher Q^2, and better agreement is indeed seen at higher Q^2. The analysis of new $n\pi^+$ data at high Q^2 [15,16] using the unitary isobar model (UIM) and

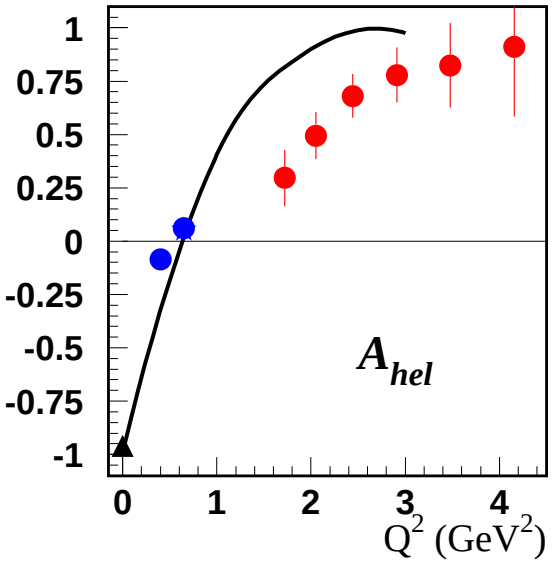


Fig. 4. The helicity asymmetry for the $D_{13}(1520)$ state. The full red symbols are preliminary results from the $n\pi^+$ analysis, while the blue points include $p\pi^0$ and $n\pi^+$ data sets. The curve represents a relativistic quark model calculations [17].

dispersion relations (DR) approaches result in the behavior shown in Fig. 3. A large positive amplitude $A_{1/2}$ is peaking near $Q^2 = 2$ GeV^2, followed by a smooth falloff. Both results are quite close and give a consistent behavior, indicating that the model-dependence is reasonably well under control. At large Q^2 the $A_{1/2}(Q^2)$ amplitudes drops somewhat faster than the LC models predict, which might indicate that the point-like coupling to the quarks is not yet realized at these Q^2, and (constituent) quark form factors are be needed to describe this transition.

3.2 The $D_{13}(1520)$ resonance

The $D_{13}(1520)$ is predicted in the CQM to rapidly change its helicity structure from helicity 3/2 dominance at the real photon point to helicity 1/2 dominance when Q^2 increases. Indications of such behavior have been seen in previous analyses, but no systematic study has been done in a large Q^2 range. Figure 4 shows the helicity asymmetry

$$A_{hel} = \frac{A_{1/2}^2 - A_{3/2}^2}{A_{1/2}^2 + A_{3/2}^2}$$

extracted from the $n\pi^+$ electroproduction data at high Q^2. The lower Q^2 data come from the analysis of $p\pi^0$ and $n\pi^+$ data in [13]. $A_{hel}(Q^2)$ shows the rapid switch in helicity dominance. The transition appears to occur in the range $Q^2 = 0.5 - 1.0$ GeV^2, and the asymptotic value is approached at $Q^2 > 3$ GeV^2.

4 New photocoupling amplitudes from π^0 data analysis in full resonance region.

New π^0 photoproduction data from CLAS have just been published [23] that cover a large angle and energy range with high statistics. The SAID analysis pacakge was used to determine new photocoupling amplitudes from these data. The $S_{11}(1535)$ amplitude determined from the $p\pi^0$ data set now agrees very well with the analysis of $p\eta$ data. This result is also consistent with the agreement found between these two channels in low Q^2 electroproduction [13], and will hopefully lead to a revision of the large uncertainties given in the Review of Particle Properties (RPP) for the $S_{11}(1535)$ photocoupling amplitude. Another result of the GWU analysis is that the $A_{1/2}$ amplitude for the transition to the $P_{13}(1720)$ resonance was found as $A_{1/2}^{GWU}(0) = 96.6 \pm 3.4$, while the RPP average is listed as $A_{1/2}^{RPP}(0) = 18 \pm 30$, i.e. consistent with zero. The new value of $A_{1/2}$ for the $P_{13}(1720)$ is qualitatively consistent with the strong excitation of this state found earlier in $p\pi^+\pi^-$ electroproduction data from CLAS [12]. The first precision data on the $p\eta'$ exclusive channel from CLAS have been published recently [24] in the hadronic invariant mass range from W=1.95 - 2.25 GeV, and cover the mass range of "missing baryons". While there are no clear signals of new s-channel resonances, evidence for contributions from the high energy tails of $S_{11}(1535)$ and $P_{11}(1710)$ are seen in the data. The analysis of Nakayama and Haberzettl [25] also shows sensitivity to higher mass candidate states $P_{11}(2100)$ and $D_{13}(2080)$, that may contribute to a predicted bump structure in the total cross section near an invariant mass of 2.09 GeV.

5 Search for other excited baryon states.

A major focus of the CLAS effort is dedicated to clarifying some of the ambiguous signals of baryon states, and to the search for new states that are predicted within the $SU(6) \otimes O(3)$ symmetry group of the symmetric 3-quark system. While there are states predicted that represent non-quark degrees of freedom, it is important to systematically search for predicted 3-quark states. Other contributions, e.g. gluonic excitations (hybrid baryons), and nucleon-meson molecule type states will complicate the picture, and may require special measurements and analyses approaches to separate them from the 3-quark states. The search with CLAS aims at complete or nearly complete measurements of a number of final states and using linearly and circularly polarized photon beams, in combination with longitudinally and transversely polarized targets.

5.1 A new P-wave resonance?

The CLAS collaboration has recently published data on η electroproduction in the mass range from threshold to 2.2 GeV [22]. The integrated cross section shows a small peak

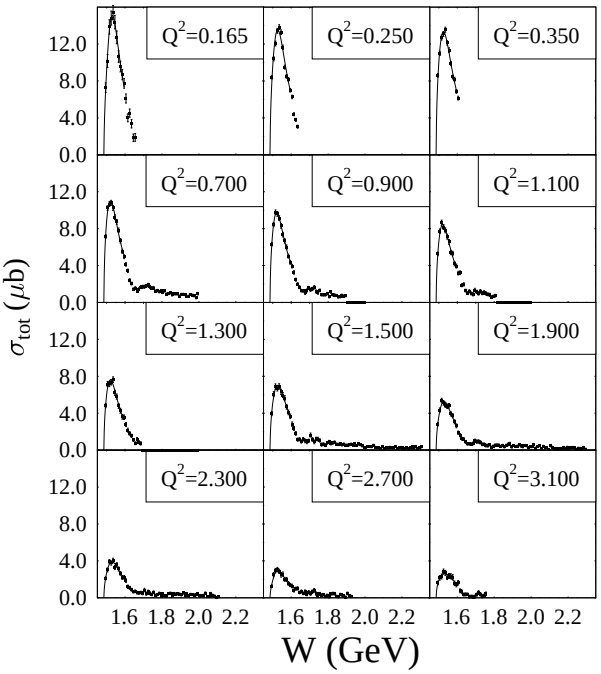


Fig. 5. The integrated cross section for η production at varies Q^2. The large peak is due to the $S_{11}(1535)$ resonance. In the mass range 1.65 to 1.7 GeV a small dip followed by a peak appears indicating a s-p interference of amplitudes from neighboring resonances.

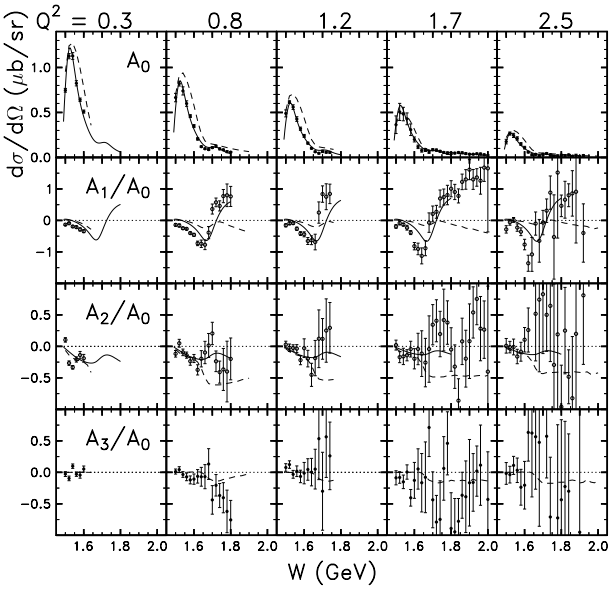


Fig. 6. Legendre coefficients A_0, and ratios of higher partial wave terms for η electroproduction data from CLAS plotted versus hadronic mass W. The most significant is the ratio A_1/A_0 that clearly shows an interference of s- and p-waves where one of the waves goes through resonance generating a zero-crossing.

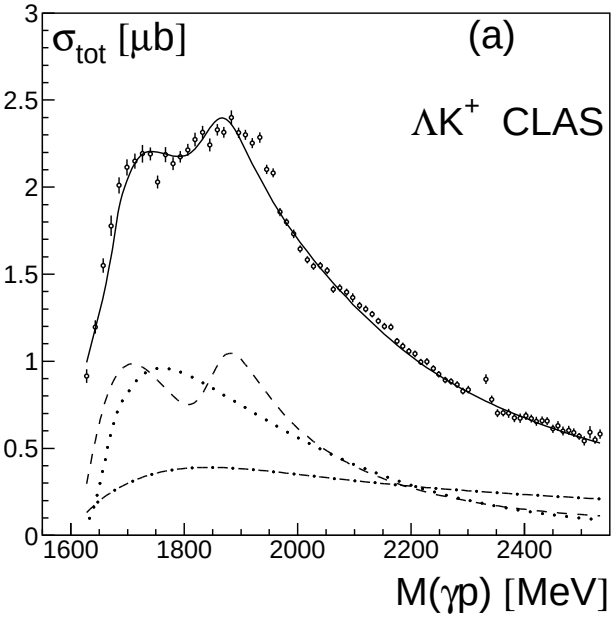


Fig. 7. Integrated cross section for $\gamma p \to K^+\Lambda$. The curves are from the Bonn-Gatchina analysis and show contributions from the $P_{11}(1710)$ (dashed-dotted), the $P_{13}(1900)$ (dashed), and from non-resonant K-exchange contributions (dotted).

structure near W=1.7 GeV and a dip near W=1.65 GeV. This pattern is shown in Fig. 5 and appears at all Q^2. To better understand this behavior we expand the response functions in a Legendre polynomial series:

$$\frac{d\sigma_T}{d\Omega_\eta} + \epsilon\frac{d\sigma_L}{d\Omega_\eta} = \sum_{l=0}^{\infty} A_l P_l(\cos\theta^*_\eta)$$

In lowest order the ratio A_0/A_1 can be expressed in terms of the multipoles E_{0+} and M_{1-} corresponding to s- and p-waves only, and reads

$$\frac{A_1}{A_0} = \frac{2Re(E^*_{0+}M_{1-})}{|E_{0+}|^2 + |M_{1-}|^2}$$

Figure 6 shows the energy dependence of the ratio A_1/A_0. It changes sign near $W = 1.65$ GeV. The observation is consistent with a rapid change in the relative phase of the E_{0+} and M_{1-} multipoles because one of them is passing through resonance. A reasonable fit to the CLAS data in that mass range is obtained with the $S_{11}(1535)$, $S_{11}(1650)$, $P_{11}(1710)$ and $D_{13}(1520)$, with a width for the $P_{11}(1710)$ of 100 MeV. Similar structures, even more pronounced have been observed in η photoproduction off neutrons, and have been discussed at this conference [26,27] as a possible new resonance. Could the observed structure be a new resonance? I think it is more likely, that the new data will merely confirm the existence of the 3-star $P_{11}(1710)$ state, and better define its poorly determined properties such as mass, width, and photocoupling.

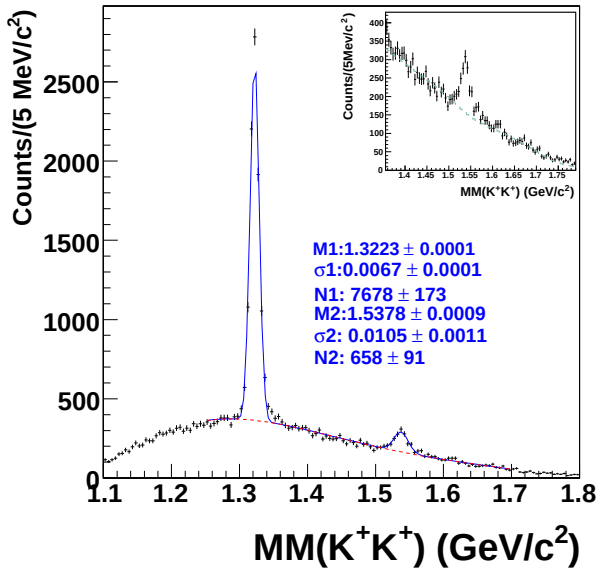


Fig. 8. Missing mass for the $\gamma p \to K^+K^+X^-$ showing the ground state $\Xi^-(1320)$ and the first excited state $\Xi^-(1530)$. The inset highlights the mass range around the 1530 MeV state.

5.2 Photo- and electroproduction of K-Hyperons

A large number of cross section data on $K\Lambda$ and $K\Sigma$ production have been published and are now being used by various groups for phenomenological analyses. The integrated cross section from CLAS [28,29] is shown in Fig. 7. These data were used in a fit by the Bonn-Gatchina group [31,32] who found significant contributions from the $P_{13}(1900)$, a two star state candidate in the RPP. The strongest constraints come from the polarization transfer data using a circularly polarized photon beam [30]. If the existence of the state can be confirmed, it will be strong evidence against a diquark-quark model that has no room for such a state [35]. Also, unpolarized and polarized response functions have been measured [33,34] in $ep \to eK^+\Lambda$ and $ep \to eK^+\Sigma$ that show significant structures in the hadronic mass spectrum, which are indicative of resonance excitations.

5.3 Search for new Ξ^* cascade baryons.

Production of Ξ^* cascade baryons with strangeness S = -2 provides another avenue in the search for new baryon states. The cascade spectrum should reflect the same mass splitting due to spin-spin interaction as the S=0 states. The advantages are due to the expected (and observed) more narrow widths of theses states. The disadvantages for using photon beams are the low cross section for the production of two kaons in the final state. A possible production mechanism is through t-channel production of $K^+\Lambda^*$,

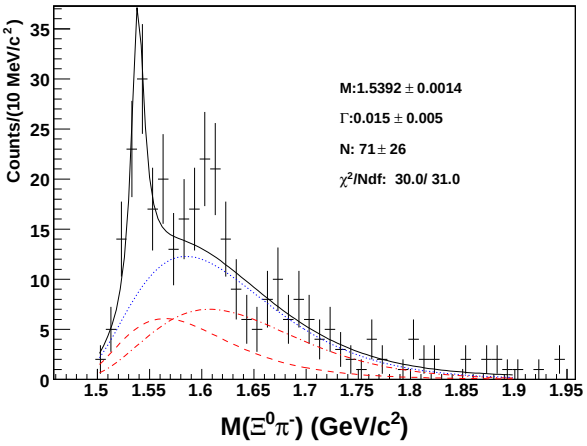


Fig. 9. The mass spectrum for $\Xi(1320\pi^-$ in the reaction $\gamma p \to \pi^- K^+ K^+ \Xi(1320)$.

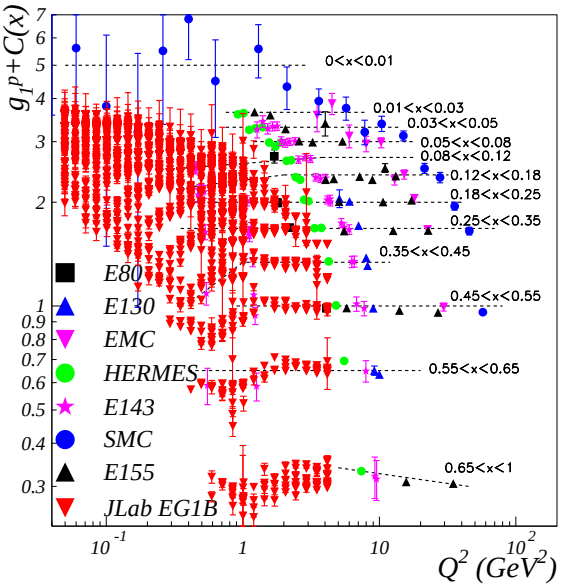


Fig. 10. The world data on structure function $g_{1p}(x, Q^2)$. The CLAS data are shown in the full red triangles.

where the excited Λ^* decays through $\Lambda^* \to K^+\Xi^*$. Figure 8 from CLAS [36] shows that one can identify the lowest two cascade states using the missing mass technique. At higher energies other states may become visible as well. Another way to search for Ξ^* states is by measuring the Ξ^0 with an additional pion. Forming the invariant mass of the $\Xi^0(1320)$ with the π^- shows in Fig. 9 again the $\Xi(1530)^-$ state. No other structure is clearly identified. Should a state at 1.62 GeV emerge at higher statistics, it could be the one star candidate in RPP. Such a state would however not be part of the 3-quark symmetry group but could be a dynamically generated $\Xi - \pi$ state prediced in dynamical models [37].

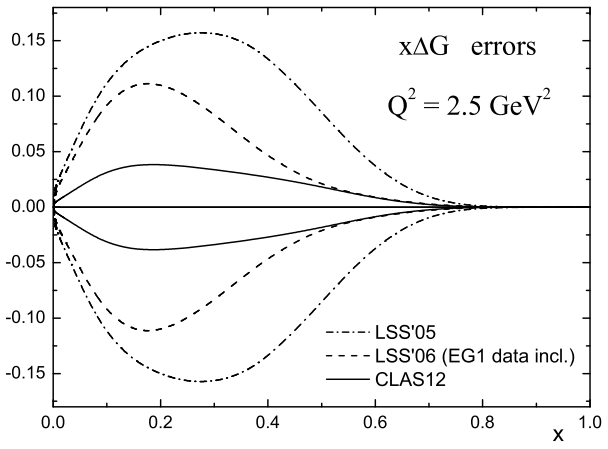


Fig. 11. Impact of the CLAS data on the uncertainties in the in the parton distribution functions from the LSS QCD analysis. The uncertainty in the polarized gluon distribution is reduced by a factor of 3 at a modest $x_B = 0.4$ (change from dashed-dotted to dashed lines) giving new constraints on the polarized gluon distribution. The uncertainties in the sea quark distribution functions are also improved significantly. The improvement in the polarized gluon distribution functions comes largely from $g_{1d}(x, Q^2)$ measured on deuterium in the same kinematics range. The projected impact of an extension of the measurements at 12 GeV with the planned CLAS12 spectrometer are shown with the solid lines.

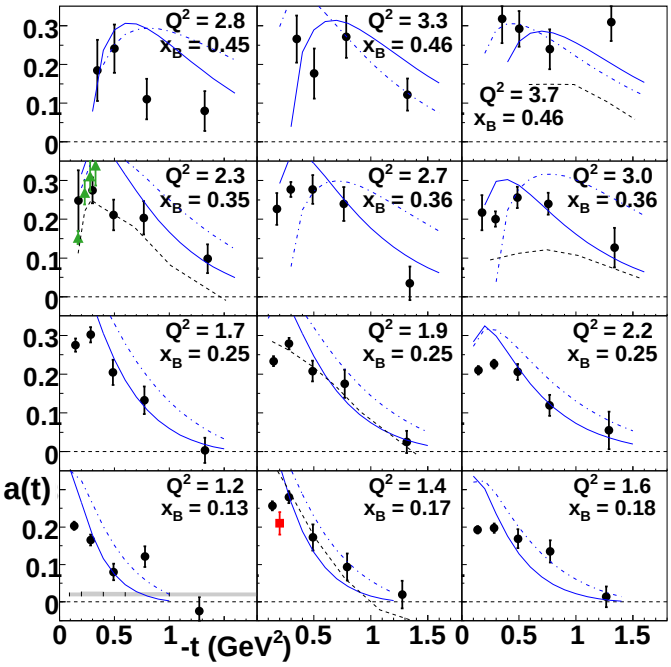


Fig. 12. The beam spin asymmetry showing the DVCS-BH interference. The red and green points represent the previous CLAS and Hall A data, respectively. The blue curve is the VGG GPD parameterization [48] in twist-2 (solid) and twist-3 (dashed-dotted). The dashed black line is a Regge model prediction [49].

6 Spin structure of the nucleon and parton distributions

The CLAS collaboration has collected very precise data on inclusive double polarization inclusive scattering resulting in high quality spin structure function $g_{1p}(x, Q^2)$ and $g_{1d}(x, Q^2)$, as well as first moments $\Gamma_1 = \int_{x_{min}}^{1} g_1(x, Q^2)dx$ for proton, deuterons and neutrons. The world data on structure function $g_{1p}(x, Q^2)$ are shown in Fig. 10. The CLAS data cover the lower Q^2 and high x_B range. The bulk of the data covers the resonance region, however the precise data in the DIS region provide strong constraints on QCD fits to extract parton distribution functions after higher twist contributions have been properly taken into account [42]. The extracted uncertainties for the polarized gluon distribution function are shown in Fig. 11, and indicate very significant reductions compared to results obtained before the CLAS data became available.

7 Generalized Parton Distributions and DVCS

The nucleon matrix element of the energy-momentum tensor contains 3 form factors that encode information on the angular momentum distribution of quark q in transverse space, $J^q(t)$, the mass-energy distribution, $M_2^q(t)$, and the pressure and force distribution, $d_1^q(t)$. For decades these form factors were of little interest as the only known process how they could be directly measured is elastic scattering of gravitons off the nucleon. Today we know that these form factors also appear as moments of the unpolarized GPDs [43]. The quark angular momentum in the nucleon is given by $J^q(t) = \int_{-1}^{+1} dx[xH^q(x,\xi,t) + E^q(x,\xi,t)]$, which at $t = 0$ results in the well known Ji sum rule, and $M_2^q(t) + 4/5 d_1^q(t)\xi^2 = \int_{-1}^{+1} dx x H^q(x,\xi,t)$. The mass and pressure distribution of the quarks are given by the second moment of GPD H, where the latter is probed by parameter ξ. A separation of $M_2^q(t)$ and $d_1^q(t)$ requires measurement of the moments in a large range of ξ. How do we access this information? The beam spin asymmetry of the deeply virtual Compton scattering (DVCS) amplitude interfering with the Bethe-Heitler (BH) amplitude is sensitive to the GPD $H(x = \xi, \xi, t)$, and has been measured at Jefferson Lab [44,45,46,47] in a wide kinematics range in Q^2, ξ, and t. The recent azimuthal asymmetries measured by CLAS were fitted with $A_{LU} = \alpha \sin\phi/(1 + \beta\cos\phi)$. The t-dependence of the leading term α for different values of Q^2 and $x_B = 2\xi/(1+\xi)$ is shown in Fig. 12. We see that α has a maximum at small t and smoothly drops to zero. The comparison of α with the standard VGG GPD parameterization [48] shows qualitative, even quantitative agreement in some kinematics, especially at large $-t$, however the theoretical asymmetry exceeds the data at small $-t$. This could mean that at low momentum transfer the denominator in the asymmetry does not fully account for all contributions to the DVCS cross section.

While the elastic GPDs are currently at the center of the development of a more complex picture of the nucleon, GPDs may also be defined for transitions where the recoil baryon is not a ground state nucleon but an excited nucleon, such as the $\Delta(1232)$ or any other excited nucleon state. Measuring the DVCS with a recoiling excited state allows probing resonance transitions at the parton level, i.e. high Q^2, and small momentum transfer t, leading to what one may call "hard nucleon spectroscopy", a new tool in probing hadronic structures that is not available in direct s-channel excitations.

8 The Future

A major focus in current and future experiments is on measurements of polarization observables in many reaction channels using linearly and circularly polarized photon beams, and longitudinally and transverse polarized proton and neutron (deuteron) targets. For strangeness containing channels often the hyperon recoil polarization can also be measured. Ultimately one would like to obtain a model-independent extraction of helicity amplitudes for at least some reaction channels as a solid basis in the search for new baryon resonances, and in the determination of the resonant photocoupling amplitudes. Differential cross sections including use of circularly polarized photons, have already been measured for many processes. Data taking on proton and neutron targets with linearly polarized photons has been completed, and the first double and triple polarization observables are underway using the polarized proton target FROST. A new frozen spin HD-ice target will be used with CLAS in 2010 for measurement of double and triple polarization observables with polarized neutrons [50]. These data will be extremely useful in fully coupled channel analyses currently under development at EBAC [51]. High statistics DVCS experiments are planned for 2008 and 2009 using polarized electrons and longitudinally polarized target which will provide much more stringent constraints on GPDs, and allow determination of some GPDs in specific kinematics.

Ackowledgment This work was supported in part by U.S. the Department of Energy and the National Science Foundation, the French commisariat á l'Energie Atomique, the Italian Instituto Nazionale di Fisica Nucleare, the Korea Research Foundation, and a research grant of the Russian Federation. The Jefferson Science Associates, LLC, operates Jefferson Lab under contract DE-AC05-060R23177.

References

1. K. Joo, *et al.*, Phys.Rev.Lett.**88**, 122001, 2002.
2. M. Ungaro *et al.*, Phys.Rev.Lett.**97**, 112003, 2006.
3. J. J. Kelly *et al.*, Phys.Rev.Lett.**95**, 102001, 2005.
4. V. Frolov *et al.*, Phys.Rev.Lett.**82**, 45,1999.
5. N. Sparveris *et al.*, Phys.Rev.C**67**, 058201, 2003.
6. N. Sparveris *et al.*, Phys.Lett.**B**651, 102, 2007.
7. C. Alexandrou *et al.*, Phys.Rev.Lett.**94**, 021601, 2005.
8. I. Aznauryan, Phys.Rev.C**76**, 025212, 2007.
9. Z.p. Li, V. Burkert, Zh. Li, Phys.Rev.D**46**, 70, 1992.
10. H. Egiyan *et al.*, Phys.Rev.C**73**, 025204, 2006.
11. K. Joo et al., Phys.Rev.C**72** 058202, 2005.
12. M. Ripani *et al.*, Phys.Rev.Lett.**91**, 022002, 2003.
13. I. Aznauryan *et al.*, Phys.Rev.C**71**, 015201, 2005.
14. I. Aznauryan *et al.*, Phys.Rev.C**72**, 045201, 2005.
15. K. Park *et al.*, arXiv:0709.1946, accepted by Phys. Rev. C.
16. I. Aznauryan and V.D. Burkert, arXiv:0711.1120 [nucl-th].
17. I. Aznauryan, private communications.
18. N. Mathur *et al.*, Phys.Lett.B**605**, 137, 2005.
19. N. Kaiser *et al.*, Phys.Lett.B**362**, 23, 1995.
20. R. Thompson *et al.*, Phys.Rev.Lett.**86**, 1702, 2001.
21. C. Armstrong *et al.*, Phys.Rev.D**60**, 052004, 1999.
22. H. Denizli *et al.*, Phys.Rev.C**76**, 015204, 2007.
23. M. Dugger *et al.*, Phys. Rev.C**76**, 025211,2007.
24. M. Dugger *et al.*, Phys. Rev.Lett.**96**, 062001,2006.
25. K. Nakayama, H. Haberzettl, Phys.Rev.C**73**, 045211, 2006.
26. H. Shimizu, plenary talk at this conference.
27. V. Kuznetsov, talk at this conference.
28. J.W.C. McNabb *et al.*, Phys.Rev.C**69**, 042201,2004.
29. R. Bradford *et al.*, Phys.Rev.C**73**, 035202,2006.
30. R. Bradford *et al.*, Phys.Rev.C**75**, 035205,2007.
31. N.A. Nikonov *et al.*, arXiv:p707.3600 [hep-ph].
32. A.V. Anisovich *et al.*, arXiv:0707.3596 [hep-ph].
33. D.S. Carman *et al.*, Phys.Rev.Lett.**90** 131804, 2003.
34. P. Ambrozewicz *et al.*, Phys.Rev.C**75** 045203, 2007.
35. E. Santopinto *et al.*, Phys.Rev.C**72**, 022201, 2005.
36. L. Guo *et al.*, Phys.Rev.C**76**, 025208, 2007.
37. A. Ramos, talk presented at this conference.
38. R. Fatemi *et al.*, Phys.Rev.Lett.**91**, 222002, 2003.
39. J. Yun, *et al.*, Phys.Rev.C**67**, 055204, 2003.
40. P. Bosted *et al.*, Phys.Rev.C**75**, 035203, 2007.
41. V. Dharmawardane, *et al.*, Phys.Lett.B**641**, 11, 2006.
42. E. Leader, S. Sidorov, D. Stamenov, Phys.Rev.D**75**, 074027, 2007.
43. K. Goeke *et al.*, Phys.Rev.C**75**, 094021, 2007.
44. S. Stepanyan *et al.*, Phys.Rev.Lett.**87**, 182002, 2001.
45. S. Chen *et al.*, Phys. Rev. Lett.**97**, 072002, 2006.
46. F.X. Girod *et al.*, arXiv:0711.4805 [hep-ph], subm. to Phys. Rev. Lett..
47. C. Munoz-Camacho *et al.*, Phys.Rev.Lett.**97**, 262002, 2006.
48. M. Vanderhaeghen, P. Guichon, M. Guidal, Phys. Rev. D**60**, 094017, 1999.
49. J.M. Laget, arXiv:0708.1250, 2007.
50. A. Sandorfi, plenary talk at this conference.
51. T.-S. H. Lee, plenary talk at this conference.